MegaDrive

» Fuel cells for large material handling vehicles «

REPORT-3

DESIGN OF 100KW-1MW FUEL CELL SYSTEMS

DECEMBER 2014

Project no.: 64012-0130

Report organizations:
Dept. of Electrical Engineering (DTU Elektro)
Technical University of Denmark

Department of Energy Technology
Aalborg University

SUPPORTED BY

Table of content

1. Summary 3

2. Fuel Cell Stack simulation 4

2.1 Thermal system modelling 4

2.1.1 Air compressor model.....7

2.1.2 Stack Cooling.....10

2.2 Membrane hydration 11

3. Fuel cell system design for 10+ tons material handling vehicles 13

3.1 System designing 13

3.2 System cost analyses.....16

3.3 Designing a joint air compressor 18

4. Fuel cell system design for MW CHP/Balancing.....20

4.1 Power Conditioning for forklift.....20

4.1.1 Power conditioning system 20

4.1.2 Lead acid battery modeling.....21

4.2 Power conditioning system MW CHP/Balancing.....23

5. List of publications.....25

1. Summary

An advanced scalable thermal numerical model of 100kW configurations was developed (including stack subsystem, cooling system and interface with the control system). The motivation for developing such models is the ability to identify optimum operational parameters and to enable parametric optimization of the systems to obtain optimum components for the given duty.

The modelling is also important in terms of identifying undesirable operational modes at a system level and from a stack and cell perspective. Eventually, the studies will lead to systems with improved lifetime and a better understanding of the maintenance and system adjustments needed throughout the system lifetime. The modelling is based on base stack specifications from Ballard.

To utilize the low-temperature waste heat, a potential fuel cell cooling and heat pump interface design is analyzed. This is to enable a system where heat is provided at sufficient temperature for infusion in the Danish district heat system.

System is optimized in terms of strategy of system operation, efficiency and capital cost. An efficiency-based approach is developed to study the optimal strategy of operation that yields to maximum system efficiency when operating multiple stacks in parallel. The optimal operational strategy is achieved through the estimation of the fuel consumption and ancillary equipment electricity use. The strategy is tested using the VDI profiles. The resulting objective function is modified according to different stack size and the results suggest that small stacks produce higher efficiency when operating at low load.

In the configuration with multiple stacks in parallel, components such as cooling heat exchanger, humidifier and compressor were duplicated according to the number of stacks. This designing choice gives more flexibility when operating multiple stacks independently however the overall system cost increases when same components are duplicated.

With the aim to reduce capital cost, we consider the option of using a single cooling heat exchanger for multiple stacks. This configuration leads to potential cost reduction for the cooling heat exchanger unit. Also we investigated the option of using a single scroll compressor instead of multiple screw compressors. This option may lead to a cost reduction which is difficult to estimate since the price of scroll compressors are a sensitive information.

2. Fuel Cell Stack simulation

2.1 Thermal system modelling

This work attempts to address the need for a control–oriented dynamic model of a PEM fuel cell system for studying temperature variations over fast load changes. For this reason, a temperature dependent cell polarization and hydration model integrated with a thermal management model was simulated in dynamic condition.

The system energy balance was reduced to a first order differential equation assuming that lumped analysis applies in terms of the thermal management. The first-order LTI (Linear Time-Invariant) system was used to obtain the transfer function.

The time constant, τ, was determined based on experimental data at different stack loads. A feed-forward control was used to vary cathode air and hydrogen mass flow rate based on the current drawn from the fuel cell. Coolant mass flow rate was also controlled based on the current reference input. A feedback PID control was used to change the radiator-fan air mass flow rate. In order to reduce cell starvation, current ramp up and down was limited to 20A/sec. Faster changes of the external load were assumed handled by an external electricity source (e.g. a battery). Few and rapid changes in external load were imposed to study the thermal controls.

It was observed that the thermal management strategy greatly influences cell temperature and efficiency which is reduced with increases stack load. Slow temperature controls are not recommended as they affect the stability of fuel cell operations. For this reason a feed-forward control of the coolant mass flow depending on stack current input was adopted. With very high variations in coolant flow rates, power consumed by liquid coolant pumps is minimal and had no considerable effect on system efficiency. On the other hand, once the coolant thermal inertia was dissolved, the air radiator fan would increase the power consumption with the result to reduce system efficiency.

An important requirement for fuel cell systems in automotive applications is to meet fast changing loads still providing proper stack cooling and hydration. In this regard, knowledge of the stack in terms of transient behavior is of critical importance. The dynamic behavior of a Proton Exchange Membrane Fuel Cells (PEMFC) system is strongly dependent on the reactant flows and the water and thermal management. Proper thermal and water management is in fact, also essential to achieve optimum performance from PEMFC stacks. Mathematical models play an important role in supporting the design and enhancing the understanding of

the effect of parameters on the performance of the stack and fuel cell auxiliary systems.

In order to describe dynamics of stack temperature under various load conditions, experimental data are to be combined with physical phenomena models with good level of approximation. The model needs to be able to be integrated with a complete fuel cell stack thermal system. In this way, it is possible to determine stack temperature and other operating parameters to fully assess the performance of the thermal system especially in highly dynamic operating conditions such as automotive applications.

In the present work-package, control-orientated system-level dynamic models are developed for stack temperature dynamics by explicitly taking into account the heat loss to the surroundings in addition to convection, the sensible heat of coolant and reactants. These models are integrated with first-principle based models of an air compressor and a semi-empirical voltage–current model. The control analysis allows estimating the thermal behavior of the stack depending of the electrical load.
The Ballard FCvelocity 9SSL 21kW stack used in this study consists of 110 cells. The active cell area is of 285.8 cm2. Liquid cooling is provided by a mix of water and ethylene glycol. The stack weights approximately 17 kg. This stack is designed for automobile applications.

The fuel cell system considered in this study is simplified in figure 1. The stack is fueled by hydrogen stored in a pressure tank. Depleted anode gas is recycled by means of a compressor and an ejector. There is no external humidification apparatus for fuel as steam is fully provided by anode gas recirculation. Cathode air is first compressed and cooled down to 65°C, thereafter it is humidified by a Nafion selectively permeable membrane humidifier. Water for the humidifier is provided by depleted cathode air. Finally, water from the air is collected in a water tank.

To avoid starvation and simultaneously match an arbitrary level of current demand, adding a rechargeable auxiliary power source which can respond quickly to the increase in current demand is necessary. Batteries or ultra-capacitors are power sources that respond relatively quickly to current demand. They can be used in parallel with a fuel cell to cover the high peaks in demand and can be recharged by the fuel cell itself, when the demand is lower. In order to reduce stack faults and degradation, fuel cell load ramp up and down is limited to 20A/sec.

Different control schemes for each fuel cell stack parameter are adopted in this study. The feed-forward control algorithm is used to control cathode air and hydro-

gen mass flow rate based on the current drawn from the fuel cell. The coolant mass flow rate is also based on the current reference input. In these cases, lookup tables were implemented in Matlab/Simulink to relate parameters with current load. Coolant temperature is reduced by means of a radiator-fan which is controlled by a PID controller. In figure 1, a simplified outline of the PEM fuel cell system is given.

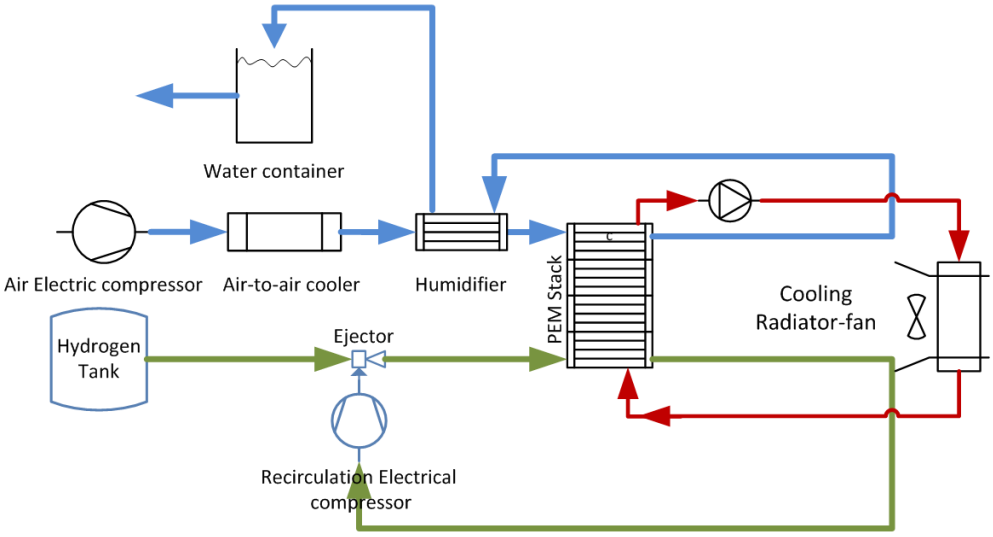

Figure 1 System piping and instruments diagram

The operating parameters that must be set in the program are air and fuel inlet stoichiometry, inlet pressure, pressure drop, relative humidity, and the operating temperature of the stack. All simulations are performed under the MATLAB/Simulink environment.

We assume an averaged stack temperature; reference stack temperature is set to 65°C. We also assume that the inlet reactant flows in the cathode and anode can be humidified, heated and cooled in a consistent and rapid way. Although this assumption will not be always true, especially during fast transients loads.

In figure 2 the calibration results of the model against the experimental data provided in Ballard manual is provided. It is important to mention that in order to reduce fuel cell degradation, low and high current density values are usually avoided mainly due to high degradation in these operational ranges.

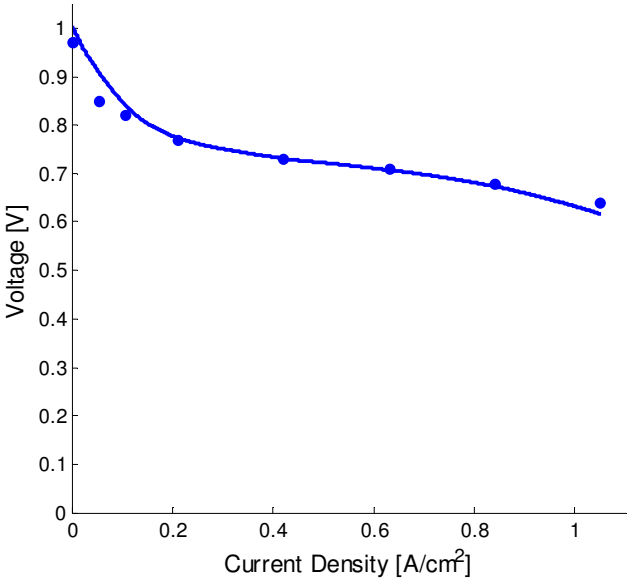

Figure 2 Fuel cell polarization curve calibration against experimental data from Ballard

2.1.1 Air compressor model

Under certain operational conditions, the pressure drop rapidly increases to very high levels in the cathode channel, with increasing costs and loss of efficiency of the fuel-cell system.

The energetic cost of the air compressor is by far the largest one among ancillary units. However, operating all cells in parallel, with all cells connected to the same entering and exiting manifolds, may block some cells where flooding is occurring. As the gases will take the path of least resistance, these cells will remain flooded.

Again, because of the usual electrical series connections, flooding of a single cell can reduce the whole stack's current as the flooded cell will work as an electrical resistance. Any approach to manage a membrane's water content based on feedback control suffers from the fundamental problem that the liquid water content in each cell is difficult to measure: both dry-out and flooding will result in a drop in voltage.

For this reason a feed-forward control of the air mass flow rate based on the stack current reference was used.

Table 1 Cathode inlet pressure and pressure drop as a function of stack current

Fuel Cell Performance Parameter							
Stack Current [A]	15	30	60	120	180	240	300
Cathode Nominal Inlet Pressure [kPa (abs)]	108	110	117	138	158	180	200
Oxidant Pressure Drop [kPa]	8	13	12	16	30	40	53

This model is based on compressor specification sheet reported in figure 3:

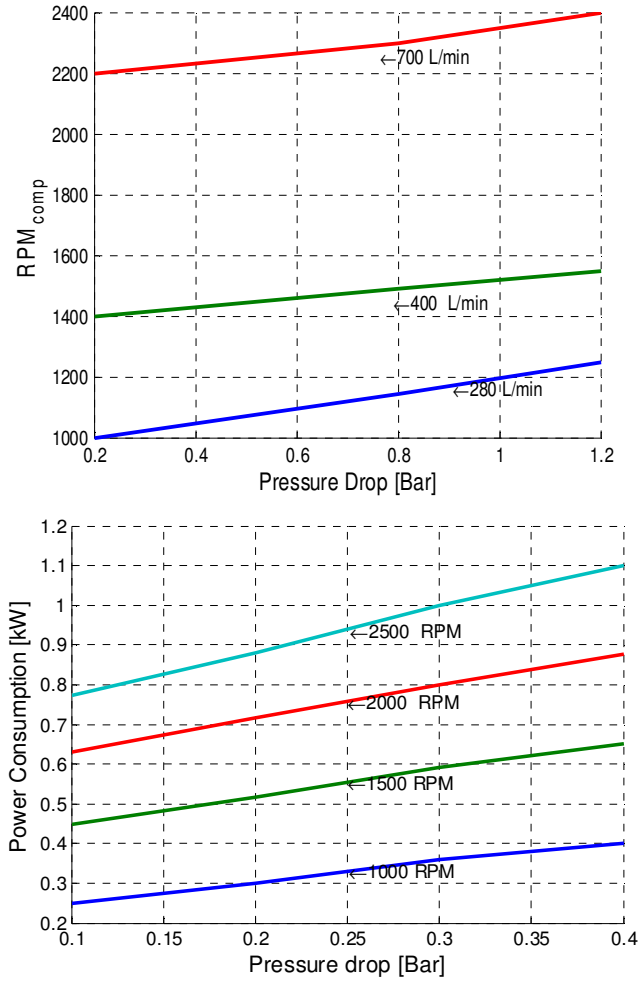

Figure 3 Compressor characteristic

(1) $RPM_{Comp} = \dot{V}_{Air} \times p_{drop}$

(2) $P_{comp} = RPM_{Comp}' \; p_{drop}$

Pressure drops p_{drop} [bar] is experimentally measured and data are reported in table 3 (Ballard 2011). Compressor revolutions per minute, RPM_{Comp} , are fitted according to compressor specification sheet. In figure 4

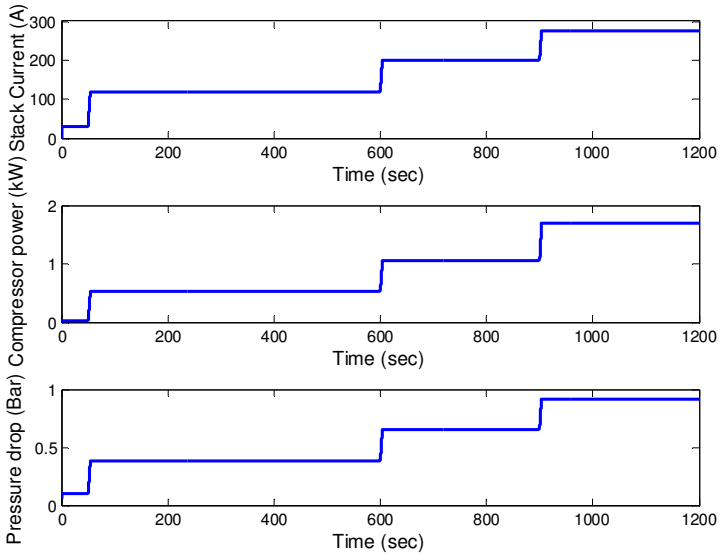

Figure 4 Air compressor power usage and cathode pressure drop at different stack load

2.1.2 Stack Cooling

Temperature changes in PEM fuel cell are considerably higher during load variations and have a negative impact as they generate thermal stresses in the stack and reduce its lifetime. Cell hydration is also of vital importance in a fuel cell. These issues pose great important on stack thermal management and control.

Assuming $\mathrm{kA_{FC}}$ as the heat transfer coefficient for the fuel cell when heat is transferred to the coolant, the time constant, τ , assumes the following form:

$$\tau = \frac{MC_{FC}}{kA_{FC}} \qquad (1)$$

The time constant says that larger stack thermal mass lead to slower changes in temperature, while larger surface areas, A_s, and better heat transfer, K, lead to faster temperature changes.

The time constant calculation is shown in table 4. An average value of 140 kJ/K was used for MC_{FC} based on Ballard Mark V stack. kA_{FC} was calculated as $\mathrm{kA}_{FC} = \dot{\mathrm{Q}}_{Coolant} / (\dot{\mathrm{V}}_{Coolant} \Delta \mathrm{T})$ where coolant heat flow rate $\dot{\mathrm{Q}}_{Coolant}$, volume flow rate $\dot{V}_{Coolant}$, and $\Delta \mathrm{T}$ where experimentally determined as reported in table 2. Coolant is a mix of water and ethylene glycol. Coolant mass flow rate was calculated assuming a coolant heat capacity, $\mathrm{C_{P,Coolant}}$, equal to $3558.78\ [\mathrm{J\ L^{-1}K^{-1}}]$.

Table 2 Time constant τ calculation based experimental values of coolant temperature

Fuel Cell Perfomance Parameter							
Stack Current [A]	15	30	60	120	180	240	300
Coolant Inlet Temperature $T_{\mathrm{Coolant,in}}$ [C]	60	60	60	60	60	60	60
Coolant Outlet Temperature $T_{\mathrm{Coolant,out}}$ [C]	61	63	66	67	68	68	70
$\dot{V}_{Coolant}$ [l/s]	0.15	0.16	0.18	0.20	0.21	0.24	0.26
$\dot{Q}_{Coolant}$ [W]	521.95	1722.45	3789.39	4863.05	6113.55	6724.9	9246.74
$\mathrm{kA_{FC}} = \dot{Q}_{Coolant} / (\dot{m}_{Coolant} \cdot \Delta T_{Coolant})$ [W/k]	521.954	574.15	631.56	694.721	764.193	840.61	924.67
τ [s]	268.22	243.83	221.67	201.52	183.2	166.54	151.40

2.2 Membrane hydration

Polymer membrane (PEM) fuel cell requires good hydration in order to deliver high performance and ensure long life operation. Water is essential for proton conductivity in the membrane which increases by nearly 6 orders of magnitude from dry to fully hydrated. Adequate water management in PEM fuel cell is crucial in order to avoid an imbalance between water production and water removal from the fuel cell.

In this work-package, a novel mathematical zero-dimensional model has been formulated for the water mass balance and hydration of a polymer electrolyte membrane. This model incorporates all the essential fundamental physical and electrochemical processes occurring in the membrane electrolyte and considers the water adsorption/desorption phenomena in the membrane. The effect of diffusivity model, surface roughness and water content driving force is considered.

The model is validated against available experimental data. In the results it is shown that the fuel cell water balance calculated by this model shows better fit with experimental data-points compared with model where only steady state operation were considered. We conclude that this discrepancy is due to a different rate of water transport when membrane absorption/ desorption is considered in the model. The model becomes useful when studying fuel cells in dynamic conditions.

Many reactions occur simultaneously in a fuel cell. These can be briefly summarized as follows: At the cathode side, hydrogen is fed to the anode channel; the gas diffuses through the anode GDL from the anode gas flow channel to the anode catalyst layer. Finally hydrogen splits in protons and electrons at the anode catalyst layer. Protons migrate through the PEM from the anode catalyst layer to the cathode catalyst layer. In parallel, the electrons transport through the external load resistance from the anode catalyst layer to the cathode catalyst layer).

At the cathode side, oxygen (or air) is fed to the cathode flow channel. Oxygen is distributed through the cathode Gas Diffusion Layer (GDL) from the cathode gas flow channel to the cathode catalyst layer. Finally, oxygen is reduced to water at the cathode catalyst layer.

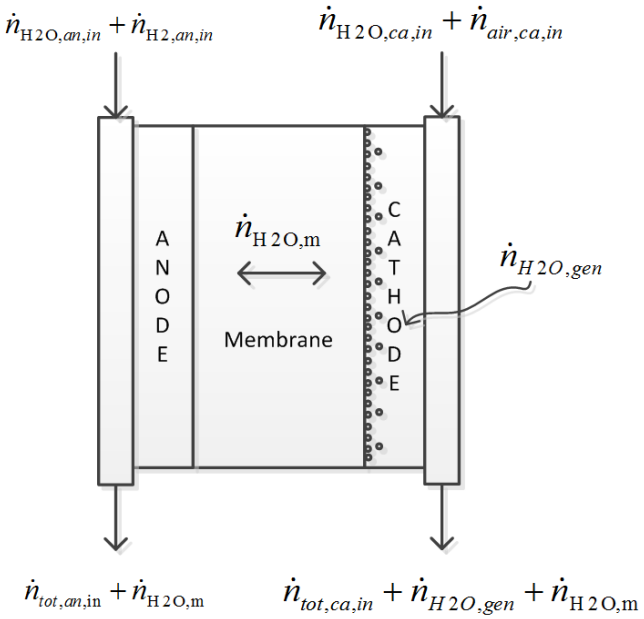

Figure 4 Water balance in fuel cell

In the following figure we depict some of modeling results. Only cathode outlet mass flow rate was used for validation. In Dynamic conditions, including adsorption/desorption phenomena gives better results than considering membrane in equilibrium condition. Water flux through the membrane is lower when introducing adsorption/desorption.

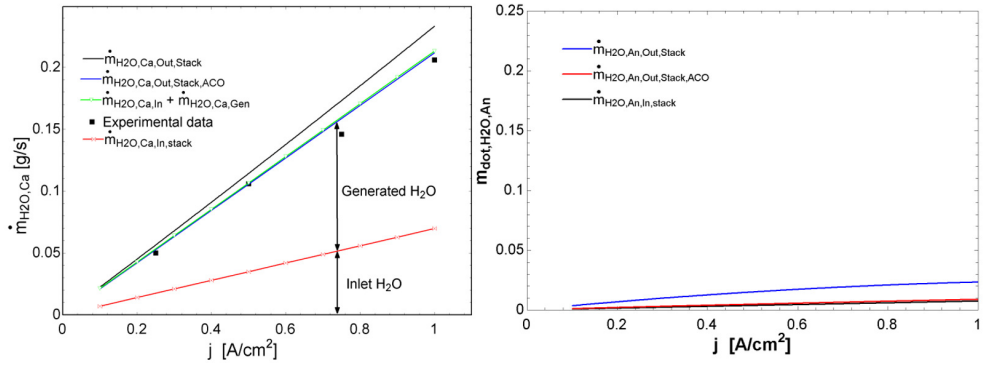

Figure 5 Outlet Cathode and Anode mass flow rate with ;

3. Fuel cell system design for 10+ tons material handling vehicles

3.1 System designing

In the configuration with power output up to 100kW multiple stacks were put in parallel. In Figure 5 the schematics of the fuel cell stack in parallel is shown. Also components such as cooling heat exchanger, humidifier and compressor were duplicated according to the number of stacks. This designing choice gives more flexibility when operating multiple stacks independently.

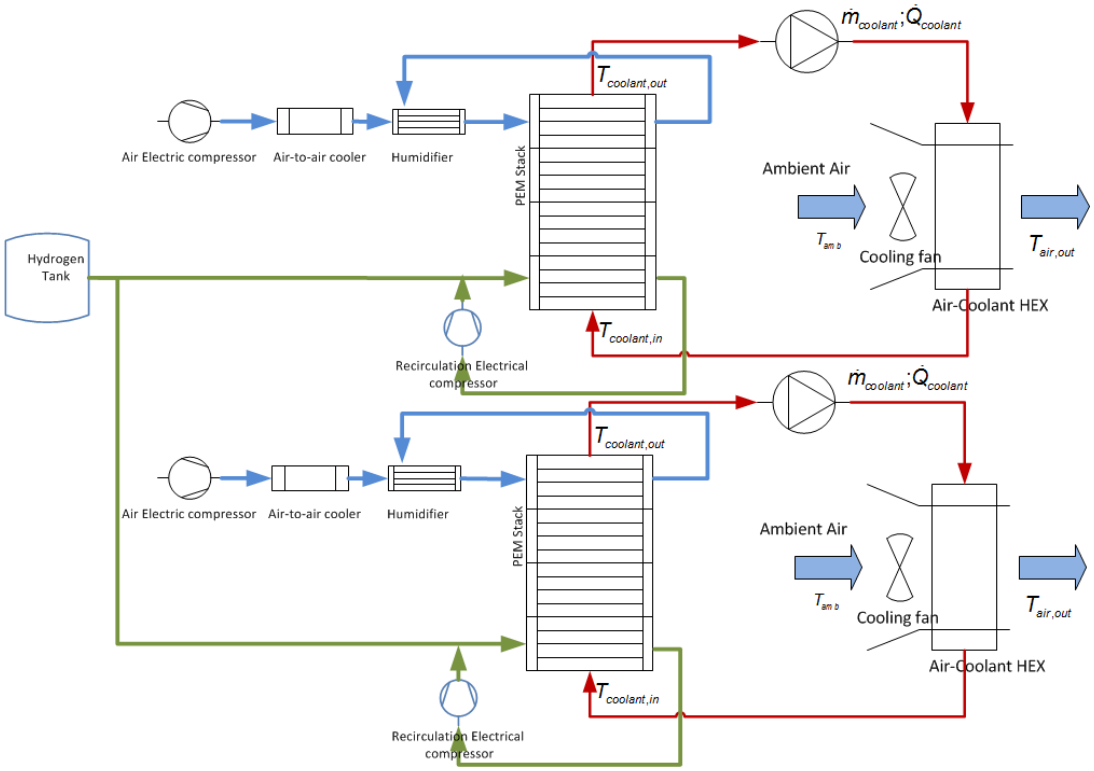

Figure 5 System with multiple stack in parallel

An option is to operate stack of different size. In the table below the maximum power of different Ballard *FCvelocity 9SSL* is shown. An advantage of this strategy is that small stacks reach higher efficiency at small loads compared to large stack. Also they have less thermal inertia and faster time of response.

Table 3 Stack maximum power

Stack Number of Cell	Max Power
20	3.8
25	4.8
55	10.6
75	14.4
90	17.3
110	21.2

For instance in the case of two stacks with 10 and 20 kilowatts we can plot the stack efficiency plot. In this evident that at low loads the small stack reaches higher efficiencies.

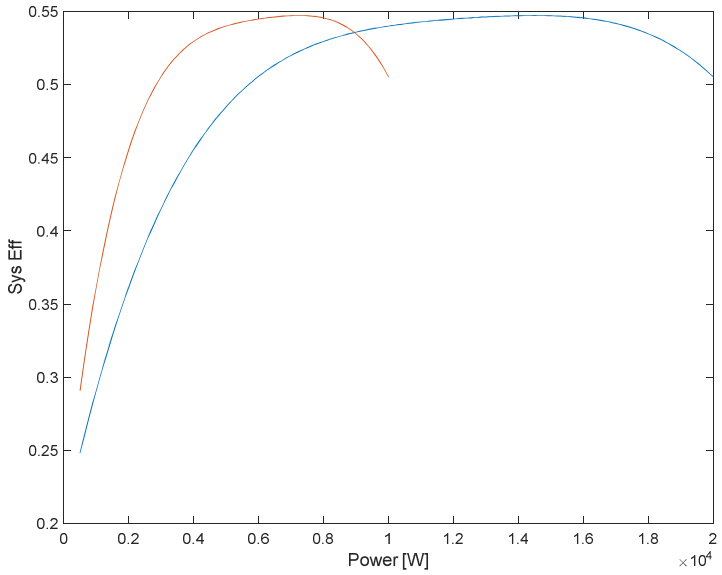

Figure 6 Stack efficiency versus load.

On the basis of this consideration a strategy of operation for multiple stack operating in parallel was defined following the rules below.

- Smallest stack start up at low loads;
- When it reaches highest efficiency (70% of the load), second smallest stack starts up;
- If the requested power is more than 70 % of max, distribute the power across the stacks proportionally the stack size.

In the figure below we consider the power output of a system including three stacks.

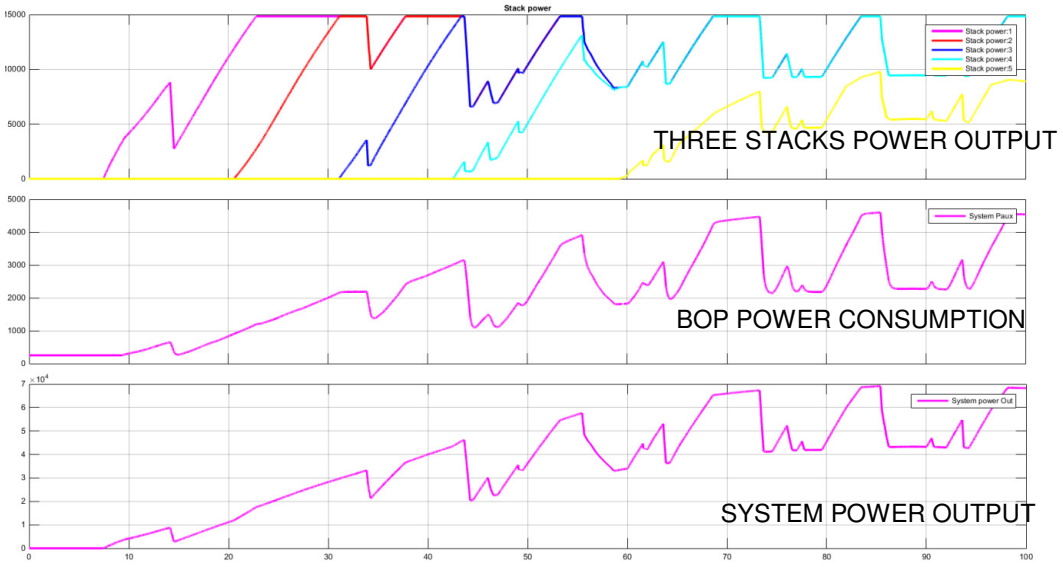

Figure 8 System power output

The graph output is produced by a Simulink code. Each stack power output can be modified using a mask and imposing stack number of cells.

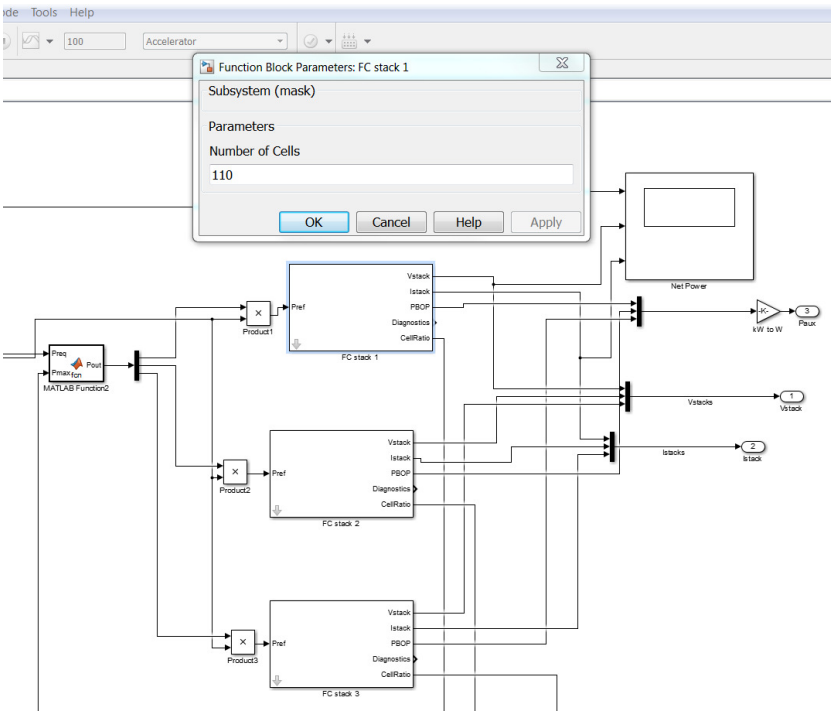

3.2 System cost analyses

Some consideration can be done on the system cost optimization. We focused on the cooling system cost and include only the cost for the heat exchanger cooler and fans.

We assume that the cost function follows a power-law behavior - here based on two real costs to fit the power law function. The fitting results are shown in figure 10.

Cooler Cost was calculated based on aluminum cooler from NRF for an AUDI 100. Fan cost was based on recommended cost from manufacturer for a Spal Cooling.

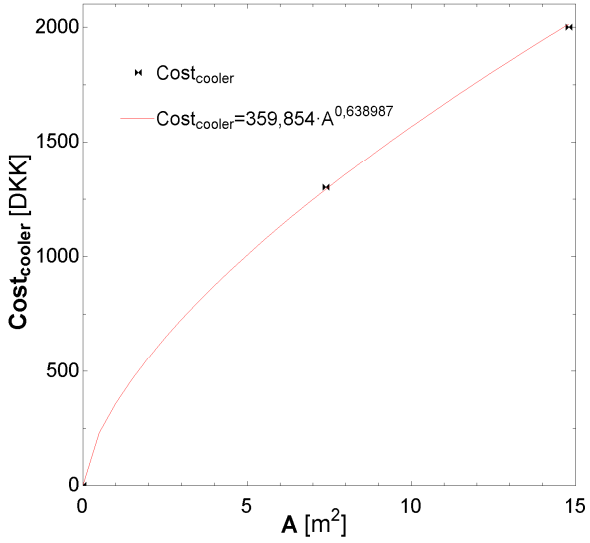

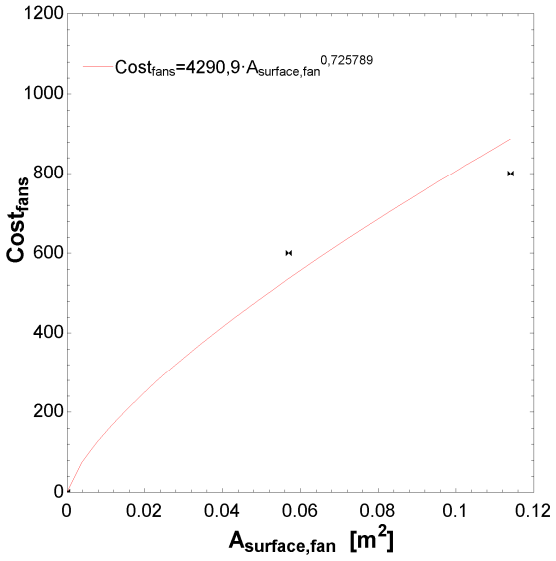

Figure 10 Cost of cooler and fan

Summing up the cost of two components, we can deduce the following curve. This function can be used as a crude estimate of the cost of the cooler including fans as function of the total heat transfer area.

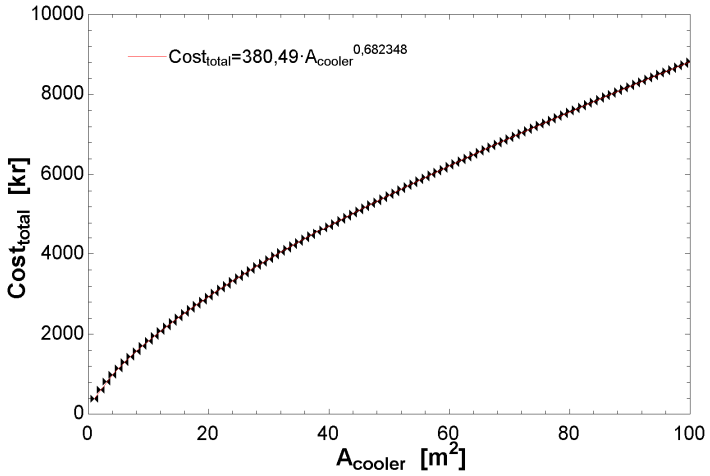

Figure 11 Cost of the cooler including fans as function of the total heat transfer area

If we assume that we scale-up the 10kW unit to 100kW it would lead to a requite heat exchanger area about 10 times larger. If we use ten units with each their cooler, the “production cost” of the 10 cooling units will be 10x1490kr=14900kr. whereas it with a single joint scaled-up cooler of roughly 74m^2 would be 7175 kr. (i.e. half the cost). This potential saving is a relatively small fraction of the total cost, but such cost reductions could be quite relevant in reaching a competitive product.

3.3 Designing a joint air compressor

The following chart illustrates approximate feasible operational regimes of different of the most common compressor technologies. All the options can in principle be made oil-free.

Currently, a scroll compressor is used in the 10kW unit. A scroll compressor provides high efficiencies at a small scale and a very constant flow. If multiple modules are to be combined with a single air-supply compressor, it would be necessary to consider using a different technology. As shown in next figure, a screw compressor may fit better to this purpose. In fact screw compressor can accommodate larger mass flow rate for similar pressure drop.

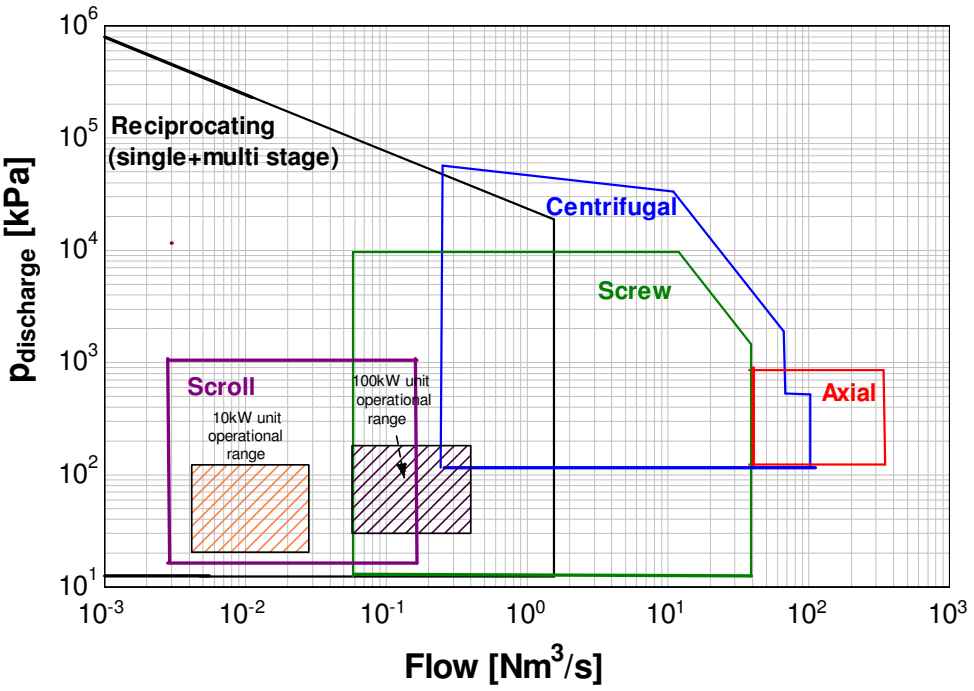

Figure 12 Compressor characteristic for different flow rate.

A multi-stage scroll compressor system would be a quite expensive option with the current technology. Scaling up a single-stage scroll compressor leads to limitations, as the inertia of the involutes would get high. Furthermore, as the compressor is fully hermetic, it is difficult to service a defect unit.

Centrifugal compressors would be an option to consider. Certain exotic high-speed centrifugal compressors could possibly fulfil the duty of the system in the operational range but would be quite expensive.

Compressor used in a fuel cell system is significantly more expensive than more ordinary compressors. However a typical screw compressor is with electrical drive has a cost of:

$$C_{Screw} = 1.81 \cdot HorsePower^{0.71} \cdot [k\$] \qquad (2)$$

This function is according to "Handbook of Turbomachinery, 2nd. Ed., New York, CRC Press, 2003". Correcting this for the "Chemical Engineering Indexes" would lead to a very crude first cost estimate.

Some disadvantages are with screw-compressors: They make more noise during operation and to some extent they have a more narrow operational range than piston based compressors, however, they are relatively cheap.

4. Fuel cell system design for MW CHP/Balancing

4.1 Power Conditioning for forklift

4.1.1 Power conditioning system

The forklift is powered by a unidirectional PEMFC, which is fuelled from a pressurized hydrogen tank.

A lead-acid battery pack is used to deliver power during fuel cell start-up, recovery of energy from regenerative braking as well as providing the instantaneous power needed to compensate for the slow dynamics of the fuel cell system.

The balance of plant (BOP) for the fuel cell is likewise powered from the battery, which allows the forklift to start up without external power. Figure 13 sketches the overall configuration of the individual components of the forklift power system.

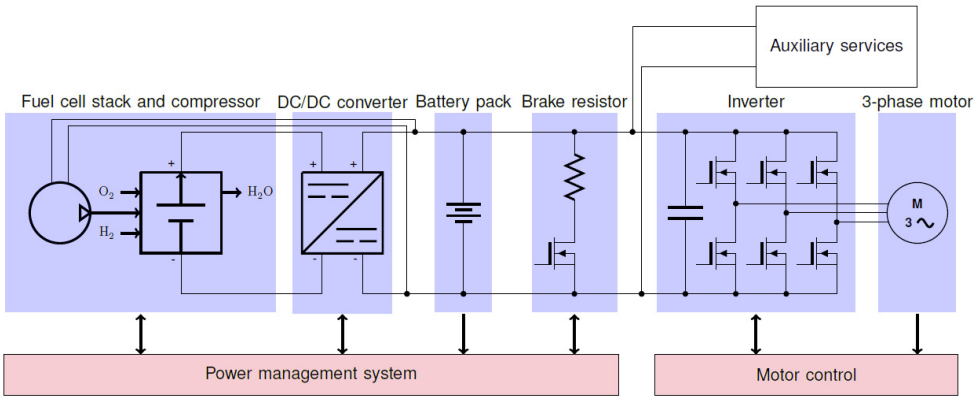

Figure 13. Forklift Powertrain block diagram

4.1.2 Lead acid battery modeling

The most critical component in the power conditioning system actually is the battery bank. The ability to accurately predict the voltage and SOC responses of batteries from arbitrary current waveforms, is a powerful tool for the vehicle designer both for dimensioning of components and optimization of the power system control algorithm.

Compared to battery packs in conventional battery powered forklifts, which have to store enough energy to last for an entire working shift, the battery pack in the fuel cell hybrid only needs to store sufficient energy to keep the forklift running for the few minutes it takes to do a cold start of the fuel cell stack.

Lead-acid batteries are well known for their ability to deliver very high currents e.g. as starter batteries in cars. Their ability to accept charge is, however, severely limited by the dissolution rate of lead sulfate. This infers that the lower limit on the size of the lead-acid batteries are limited, not by their energy content, but by their maximum charge acceptance, which will occur during regenerative braking. The results is that the current density in the battery pack will be much higher than in the corresponding battery powered forklift, which means that the battery impedance nonlinearity arising from the current through the battery becomes very significant.

In this specific case, where some of the system operation conditions are relatively well known, it is possible to make a number of simplifying assumptions which can limit both the battery model complexity, the parameter identification and the required computational power: operational SOC is limited, i.e. 30%-60%; gassing is neglected; low frequency transient response is neglected and self-discharge is neglected.

The battery is modelled using the equivalent circuit diagram in figure 14.

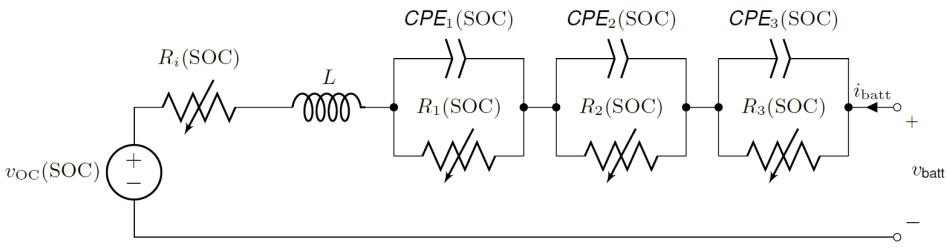

Fig. 14. Battery equivalent circuit diagram.

cy domain method for battery param-
ent dependent resistors are found by
ters of the initial frequency response
asured in the time domain.Figure 15
frequency domain measurements.

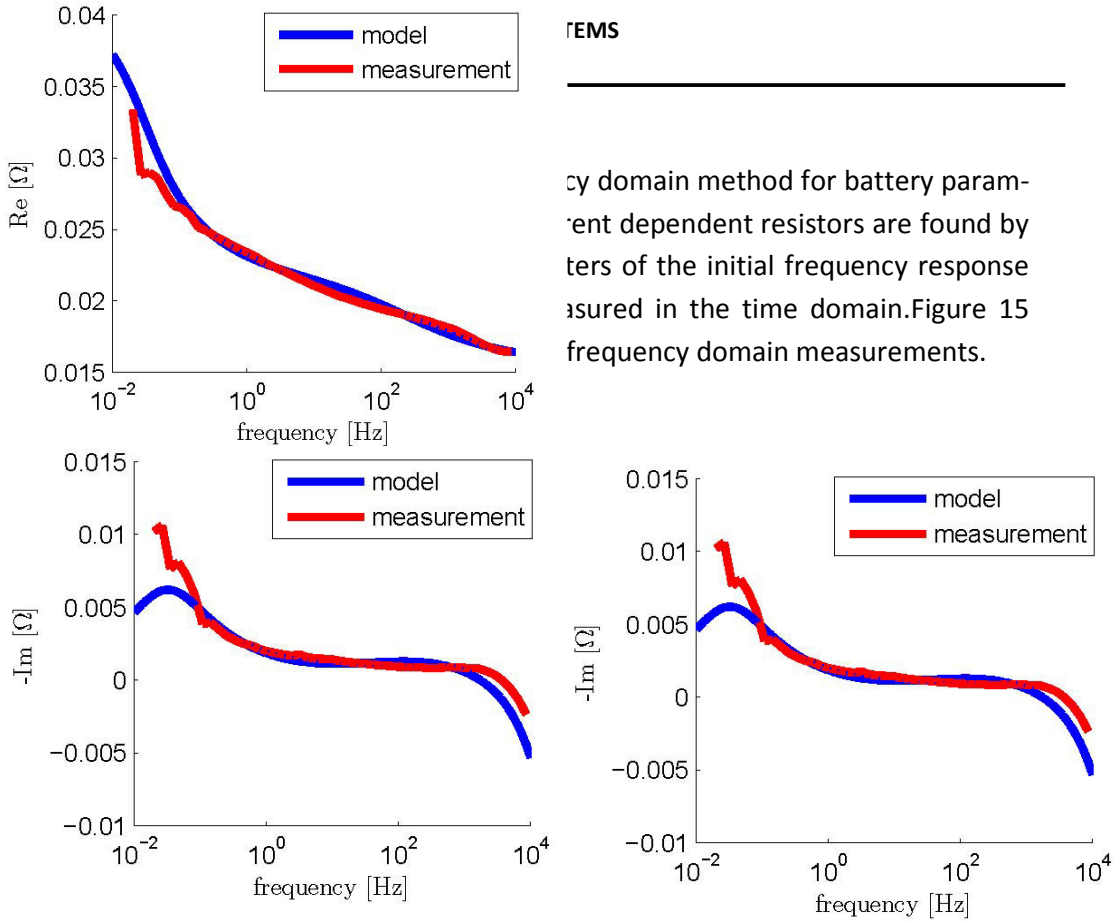

Fig. 15. Impedance measurements at SOC=57%.

Figure 16 shows independent measurement data of the battery response compared to the result of the simulation data from the battery model. The model appears to be able to predict the measurement results with good accuracy.

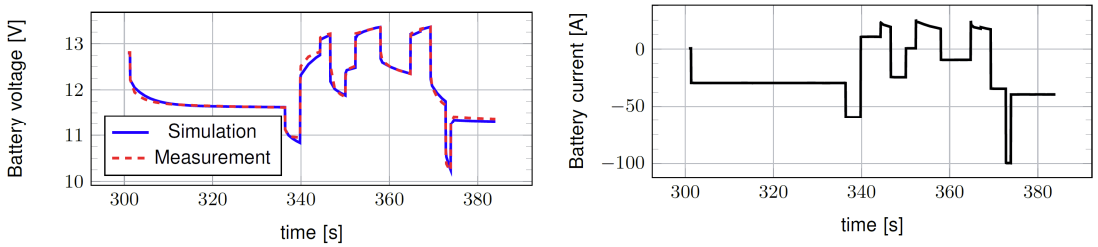

Fig. 16. Battery simulation results vs. independently measured test data.

4.2 Power conditioning system MW CHP/Balancing

Based on the investigation of the power conditioning system for MW CHP, the power conditioning system based on fuel cells and batteries can be constructed as the block diagram shown in figure 17.

In the system, only a single energy conversion stage, including an energy storage unit is adopted; therefore it provides a system size reduction and low cost due to compactness.

Additionally, the energy storage unit, as reactive power compensator, can effectively remove low-frequency current harmonics at the output of fuel cells, hence reducing the size of electrolytic capacitors and improving the lifetime of high power fuel cells, so that the system cost reduction can be even further.

Moreover, a battery service charger can be added, but not necessary, in order to maintain the batteries to extend their lifetime.

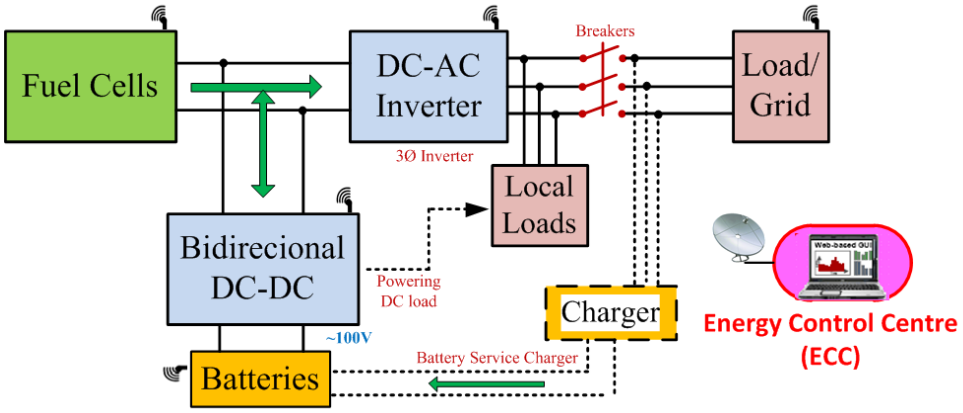

Fig. 17. Block diagram of the power conditioning system for MW CPH based on fuel cells and batteries.

Based upon the models of fuel cells and batteries given above, the system can be simulated and the main simulation results are then presented in figure 18.

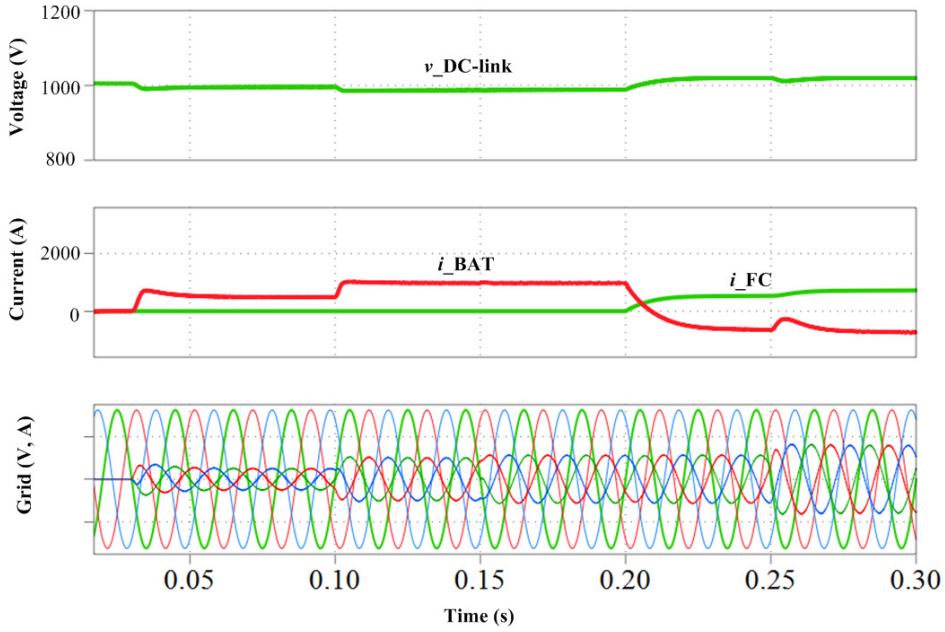

Fig. 18.MW simulation system.

In the simulation, before t=0.2s, only the batteries deliver power to the grid or load. After the fuel cells are ready for delivering power, then fuel cells will provide power to the load as well as change the batteries.

The injected active power is increased at t=0.1s; reactive power (inductive) is injected into the load or the utility grid from t=0.15s; from t=0.25s higher active power is added and at the same time, the injected reactive power is changed to be capacitive, as observed from the phase angle between phase current and voltage. Therefore, it can be seen that the proposed system can fulfill the requirements from both user side and grid service side in different operating conditions.

5. List of publications

- Liso, Vincenzo; Nielsen, Mads Pagh; Kær, Søren Knudsen; Mortensen, Henrik H. Thermal modeling and temperature control of a PEM fuel cell system for forklift applications. In: International Journal of Hydrogen Energy Elsevier Volume 39, Issue 16, 27 May 2014, Pages 8410-8420.
- Liso, Vincenzo; Nielsen, Mads Pagh. Dynamic Thermal Model And Control Of A Pem Fuel Cell System. In Proceedings European Fuel Cell Technology and Applications Conference 2013.
- Liso, Vincenzo; Nielsen, Mads Pagh; Araya, Samuel Symon; Olesen, Anders Christian. Modeling and experimental validation of water mass balance in a PEM fuel cell. In preparation.
- Z. Zhang, H. Mortensen, J. Jensen, and M. Andersen, “Fuel cell and battery powered forklifts,” in Vehicle Power and Propulsion Conference (VPPC), 2013 IEEE, Oct 2013, pp. 1–5.